Int. J. Heat Mass Transfer. Vol. 22, pp. 1049–1057
© Pergamon Press Ltd. 1979. Printed in Great Britain

0017-9310/79/0701-1049 $02.00/0

NON-ISOTHERMAL LIQUID FLOW AND HEAT TRANSFER IN SINTERED METALLIC POROUS MEDIA

B. S. SINGH* and A. DYBBS
Department of Mechanical and Aerospace Engineering, Case Western Reserve University, Cleveland, OH 44106, U.S.A.

(*Received* 11 *May* 1978 *and in revised form* 27 *November* 1978)

Abstract—This paper presents an experimental and analytical study of non-isothermal liquid flow in sintered fiber metallic porous media. The purpose of the paper is to present a self-consistent procedure for determining heat-transfer characteristics of porous metals. The analysis uses the volume averaged conservation equations. Darcy's law is assumed to hold and local thermal equilibrium is assumed to exist between the solid and liquid phases. The coupled conservation equations are solved for one and two dimensional temperature distributions using finite difference schemes. Different flow and thermal boundary conditions are used. The experiments involve the measurement of temperature distributions and effective thermal conductivities of water saturated copper and nickel sintered fiber metal wicks. The effective thermal conductivities are measured using the steady-state method of comparison and the resulting values are used in the volume averaged energy equation. The measured temperature distributions and those predicted by the analysis show good agreement. Thus the procedure presented in this paper for predicting heat transfer seems to be valid.

NOMENCLATURE

a, radius of cylinder [m];
C_p, specific heat capacity [J/kg K];
d, pore size [m];
g, gravitational constant [9.80665 m/s^2];
k, permeability [cm^2];
L, characteristic length [m];
l, axial distance [m];
P, reference pressure [N/m^2];
p, fluid pressure [N/m^2];
Pe, Peclet number $(\rho_f C_{p_f} UL)/\lambda_{\text{eff}}$;
R, dimensionless radial distance (r/a);
r, radial dimension [m];
Re, Reynolds number $(\rho_f Vd/\mu)$;
T, temperature [K];
U, characteristic velocity [m/s];
u, fluid velocity [m/s];
V, fluid velocity [m/s];
v, deviation velocity [m/s];
Z, dimensionless axial distance (z/L);
z, axial dimension [m].

Greek symbols

λ, thermal conductivity [W/m K];
μ, viscosity [kg/m s];
ν, average volume [m^3].

Superscripts

$\bar{}$, averaged property;
$'$, deviation of value from average.

Subscripts

eff, effective property;
f, fluid property;
H, high value;
L, low value;
R, reference property;
r, radial direction.

INTRODUCTION

AN UNDERSTANDING of heat transfer and non-isothermal flow in porous media is important for the design and analysis of devices in many branches of engineering. For example, metallic porous materials are commonly used in heat pipes and heat exchangers; for transpiration cooling, filters, noise reduction and boundary-layer control. For successful design these applications require the calculation of the temperature distribution in porous materials with forced convection and a knowledge of the internal heat-transfer coefficient between the porous material and the fluid flowing through it. Apparently there is no widely accepted analytical procedure for these calculations and recourse has to be made to experiments. This is due to a number of factors:

(1) The difficulty of analytically and experimentally determining the effective thermal conductivity of porous materials fully and partially saturated with a fluid.

(2) The question of what set of conservation equations best characterize non-isothermal flow in porous media and

(3) The lack of experimental data needed to verify a particular analytical model.

These difficulties are interrelated. For example, the analytical model often determines the type of measurements that must be made; and the definition of the effective thermal conductivity, which is not a thermodynamic property, determines the nature of the conduction term in the energy conservation equation.

* Presently at Energy Development Associates, Madison Hts., MI 48071, U.S.A.

The purpose of this paper is to provide a self-consistent procedure for the calculation of one and two dimensional temperature distributions in liquid saturated porous materials. The problem of determining the internal heat-transfer coefficient will be discussed in a later paper for both thermal and non-thermal equilibrium cases. In this paper, local thermal equilibrium in the porous medium will be assumed. Porous metals and water will be used for the experimental verification and the flow will be in the Darcy regime.

Effective thermal conductivity

For these studies the effective thermal conductivity of a fully saturated porous material is defined as the ratio of the total heat flux to the average temperature gradient [1]. It is not a thermodynamic property and can depend on the geometrical arrangement of the constituent phases, the porosity, the thermal conductivities of the phases, and the thermal boundary conditions. While in principle it can be evaluated, in practice this is impractical because the porous medium structure is seldom known. This is particularly true of sintered metallic porous media whose structure is extremely complex and for which a characteristic length and hence a "unit cell" is very difficult to define. Thus in this work the effective thermal conductivity of liquid saturated porous metals was experimentally determined by using the steady state method of comparison. Details of the experimental process can be found in [2,3]. It should be noted that the effective thermal conductivity thus determined is for a stagnant liquid in a porous metal in the absence of radiation and convection. It is this effective thermal conductivity that is used in the conduction term of the energy equation presented below.

ANALYTICAL MODEL—CONSERVATION EQUATIONS

The phenomena of heat transfer and fluid flow in porous media can be described by applying the well known conservation equations of classical fluid mechanics—continuity, momentum, and energy to both the fluid and solid phases of the porous media (together with appropriate equations of state). This set of equations could be solved with appropriate boundary conditions (at the boundaries of the porous material) and interfacial conditions at the solid fluid interfaces (within the porous material). For porous media commonly encountered the solid fluid interfaces are very irregular and complex, and hence difficult to describe. Thus the solution of the problem is extremely difficult and at present appears to be intractable.

To overcome this difficulty, a number of analytical approaches have been used. These can be classified as cell or phenomenological modelling, statistical, and volume averaging. Details of these approaches can be found in [4–6]. Of these three the volume averaging approach appears to be the most appropriate. It has a strong analytical basis, is sufficiently general, and lends easily to experimental verification. This approach will provide only a macroscopic picture of the phenomena and would normally require a knowledge of some properties of the porous media.

In this paper the volume averaged conservation equations applicable for flow in the Darcy regime with local thermal equilibrium are investigated. This approach was independently developed by Dybbs [7], and Slattery [4]. The equations presented below are for a steady, incompressible low Reynolds number ($Re \ll 1$) flow through a homogeneous and fully saturated porous media for the case of thermal equilibrium between the fluid and the solid phases. The equations presented here are adapted from Dybbs and Schweitzer [5].

The conservation of mass is described by

$$\nabla \cdot \bar{\mathbf{V}} = 0 \tag{1}$$

where the overbars represent the volume averaged property defined as

$$\bar{V} = \frac{1}{v}\int \mathbf{V}\,\mathrm{d}V \tag{2}$$

v being the averaging volume. The conservation of momentum is described by

$$\bar{V} = -\frac{k}{\mu}(\nabla \bar{p} - \bar{\rho} g) \tag{3}$$

which is a generalization of the empirical relationship proposed by Darcy [8]. The validity of Darcy's law for isothermal flow has been verified by numerous authors, further details of their work can be found in Scheidegger [6].

The validity of Darcy's law for non-isothermal flows has received little attention. Dybbs [7] and Dybbs and Schweitzer [5], based on their volume averaged conservation equations, have shown that Darcy's law should be valid for low Reynolds number non-isothermal flow in porous media provided that the property variations with temperature are properly taken into account. Schweitzer [9] has also proposed inclusion of an additional term in Darcy's law to represent the effect of temperature gradient. Singh, Huang and Dybbs [10] conducted experiments to study the validity of Darcy's law for non-isothermal flow in sintered metallic porous media as well as packed beds. Their results substantiate the conclusion of Dybbs [7] and Dybbs and Schweitzer [5]. Huang and Dybbs [11] using the principles of irreversible thermodynamics, demonstrated that Darcy's law should be valid for non-isothermal flow in porous media and the inclusion of any additional terms as proposed in [9] is not required.

Darcy's law is valid only for low Reynolds number flows. For $Re \geqslant 10$ the inertia effects start to become important and Darcy's law is no longer applicable. An inertia term is added to Darcy's law in order to extend its range of validity. Details of this extended

Darcy law for isothermal flow can be found in [12–15] and for non-isothermal flow in [16].

The conservation of energy is described by

$$\bar{\rho}_f \bar{C}_{p_f}[\nabla\cdot(\bar{\mathbf{V}}\bar{T})+\nabla\cdot(\overline{\mathbf{v}'T'})] = \lambda_{\text{eff}}\nabla^2\bar{T} \quad (4)$$

for details of its derivation see [5].

The experimental results of Dybbs and Schweitzer [17] have verified the applicability of a form of this equation for loosely packed beds. In addition Singh and Dybbs [18] have studied the validity of equation (4) for one dimensional flow and heat transfer in water saturated sintered metal cylinders. They measured the effective thermal conductivity and temperature distribution of the saturated porous medium; their results indicate that:

(a) For the flow rates considered ($Re \leqslant 10$) the effective thermal conductivity did not change with flow rate.

(b) The contribution of the second term $\overline{\rho_f}\ \overline{C_{p_f}}\ \nabla\cdot(\overline{T'\mathbf{V}'})$ on the LHS of equation (4) is not important and the term can be dropped.

In the paper of Singh and Dybbs [18] the data for Tegraglas (sintered glass) showed some deviation from the analytical results but this was mainly due to heat losses from the test section which became significant for the low thermal conductivity material but were insignificant for the metallic specimens. This conclusion was further substantiated by additional experiments reported in [19].

Hence the energy conservation equation used in this paper is

$$\bar{\rho}_f \bar{C}_{p_f}\nabla\cdot(\bar{\mathbf{V}}\bar{T}) = \lambda_{\text{eff}}\nabla^2\bar{T}. \quad (5)$$

Equations (1) and (3) are combined to obtain

$$\nabla^2\bar{p} - \frac{1}{\bar{\mu}}[\nabla\bar{p}\cdot\nabla\bar{\mu}] = 0. \quad (6)$$

For most fluids the viscosity is a strong function of temperature. Thus

$$\mu = \mu(T) \quad (7)$$

and

$$\nabla^2\bar{p} - \frac{1}{\bar{\mu}}\frac{\mathrm{d}\bar{\mu}}{\mathrm{d}T}[\nabla\bar{p}\cdot\nabla\bar{T}] = 0. \quad (8)$$

Thus equations (5) and (8) describe heat transfer and fluid flow in porous media with the previously mentioned assumptions. The equations are coupled by the variation of the viscosity with temperature.

Equations (5) and (8) can be non-dimensionalized by an appropriate reference temperature T_R, pressure P_R, viscosity μ_R, characteristic length L, and characteristic velocity U_R. The resulting equations are:

$$\nabla^2 p - \frac{1}{\mu}\frac{\mathrm{d}\mu}{\mathrm{d}T}[\nabla p\cdot\nabla T] = 0 \quad (9)$$

and

$$Pe\nabla\cdot(\mathbf{V}T) = \nabla^2 T \quad (10)$$

where the bars have been dropped and the

$$Pe = (\rho_f C_{p_f} U_R L_R)/\lambda_{\text{eff}} \quad (11)$$

where U_R is the Darcy filter velocity and L_R is a characteristic length of the porous medium such as a radius for a cylindrically shaped material.

In the present study the specimens used were cylindrical and the boundary conditions were azimuthally symmetric. Equations (9) and (10) become

$$\nabla^2 p - \frac{1}{\mu}\frac{\mathrm{d}\mu}{\mathrm{d}T}\left[\frac{\partial p}{\partial r}\frac{\partial T}{\partial r}+\frac{\partial p}{\partial z}\frac{\partial T}{\partial z}\right] = 0 \quad (12)$$

$$\nabla^2 T - Pe\left[u_z\frac{\partial T}{\partial z}+u_r\frac{\partial T}{\partial r}\right] = 0 \quad (13)$$

where u_z and u_r are the axial and radial velocity respectively.

Distilled water was used as the saturating fluid. The viscosity variation of distilled water with temperature can be approximated by using the Helmholtz relationship.

$$\mu(T) = 1.779/(1.0+0.03368T+0.00022T^2) \quad (0^\circ\text{C} < T < 100^\circ\text{C}) \quad (14)$$

where μ is the viscosity in centipoise.

Both one and two dimensional temperature distributions were studied. The boundary conditions for the cylindrical materials studied are discussed below and shown schematically in Fig. 1.

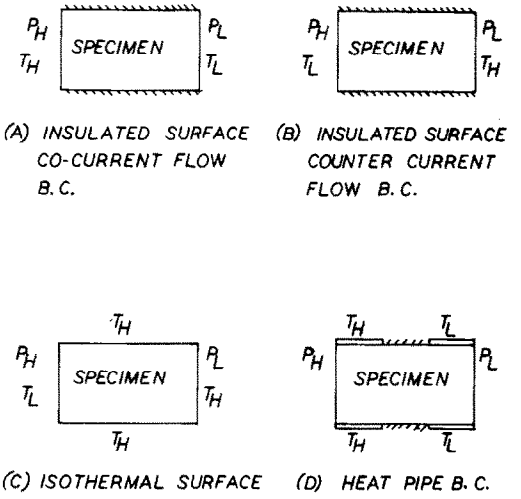

FIG. 1. Schematic diagram of the boundary conditions studied.

(A) The end surfaces are kept at constant uniform temperature while the lateral surface is insulated. The fluid flows from the high temperature to the low temperature end. This is referred to as co-current flow boundary condition shown in Fig. 1(A). At,

$$z = 0,\ T = T_H,\ p = p_H;\quad z = L,\ T = T_L,\ p = p_L$$
$$r = a,\ 0 < z < L,\ \partial T/\partial r = 0. \quad (15)$$

(B) Same as (A) but with the fluid flow in the direction of increasing temperature. Referred to as counter-current flow boundary condition, shown in Fig. 1(B).

(C) The lateral surface kept at a constant temperature. The fluid flow is opposed to the temperature

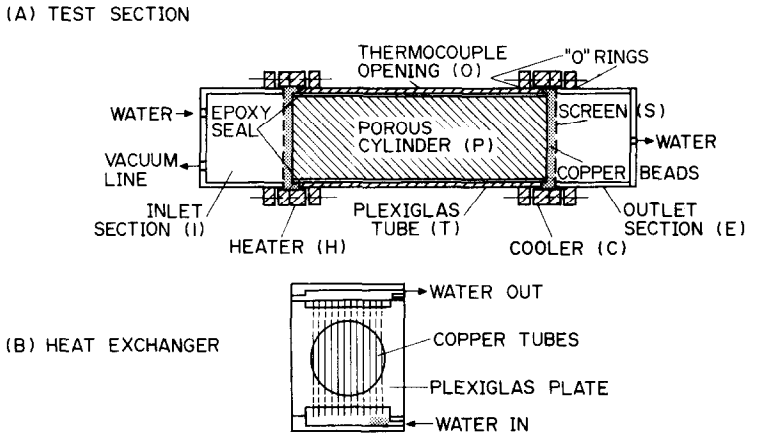

FIG. 2. Schematic diagram of the test section and the heat exchanger.

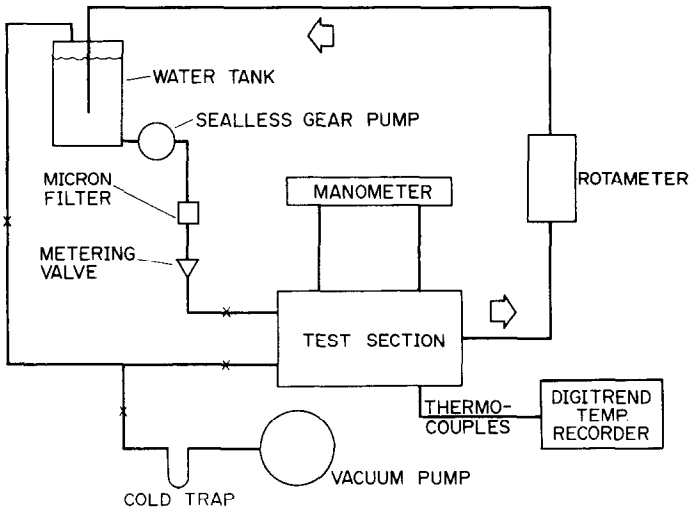

FIG. 3. Schematic diagram of the experimental set-up.

gradient. This is referred to as the constant surface temperature boundary condition, shown in Fig. 1(C).

$$\text{at } r = a,\ 0 < z < L,\ T = T_H;$$
$$z = 0,\ T = T_L,\ p = p_H,$$
$$z = L,\ T = T_H,\ p = p_L. \tag{16}$$

(D) One part of the specimen lateral surface near one end was kept at a prescribed temperature whereas an equal length near the other end was kept at another temperature. The remaining lateral surface being insulated. This is shown in Fig. 1(D) and referred to as heat pipe boundary condition

$$\text{at } r = a,\ 0 < z < l,\ T = T_H;$$
$$r = a,\ l < z < L - l,\ \partial T/\partial r = 0$$
$$r = a,\ L - l < z < L,\ T = T_L;$$
$$z = 0,\ T = T_H,\ p = p_H$$
$$z = L,\ T = T_L,\ p = p_L;\ l < L/2. \tag{17}$$

EXPERIMENTAL APPARATUS AND PROCEDURE

The experimental program was divided into the following parts:

(i) Determination of permeability which involved isothermal measurements of the pressure drop across the specimen and the fluid flow rate.

(ii) Measurement of the effective thermal conductivity of the specimen fully saturated with stagnant fluid.

(iii) Measurements of the temperature distribution, pressure drop and flow rate for the case of non-isothermal flow.

An apparatus that would permit the performance of all the above mentioned tests on each specimen with a minimal of modification from one test to another was developed and used.

This apparatus was similar to the one described in [18] and is shown for clarity schematically in Figs. 2 and 3. Details may be found in [19]. The essential

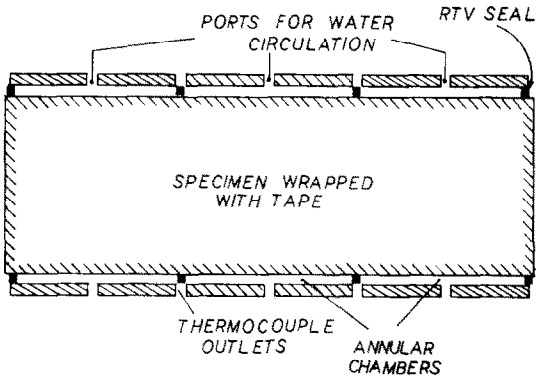

FIG. 4. Sketch of the cylindrical porous specimen contained in the Plexiglas enclosure.

difference between the apparatus used in [18] and the one employed in the present study is the change in the specimen containment to allow maintenance of two dimensional thermal boundary conditions. The specimen wrapped with lead (or aluminum) tape and containing thermocouples was contained in a Plexiglas envelope as shown in Fig. 4. The envelope was made of three pieces of Plexiglas tube which were sealed together as well as to the specimen with RTV rubber cement. There was a gap of ~0.32 cm between the specimen surface and the Plexiglas tube containing it. The gap was divided into three compartments each covering one-third of the specimen length. Water from Haake constant temperature baths could be circulated through each compartment to maintain it at a desired temperature. Thus the boundary conditions shown in Fig. 1 could be maintained on the specimen surface.

EXPERIMENTAL RESULTS AND COMPARISON WITH ANALYSIS

The experimental results for two sintered metal materials are presented in this section. In particular a detailed comparison is made between the experimental temperature distributions and those predicted by the analytical model.

Sintered specimens of copper and nickel 200 were tested under the boundary conditions shown in Fig. 1. Water was used as the saturating fluid and all tests were conducted within the Darcy regime. Some properties of the specimen and saturating fluid are given in Table 1.

The permeability was measured under isothermal conditions (~22°C) and the effective thermal con-

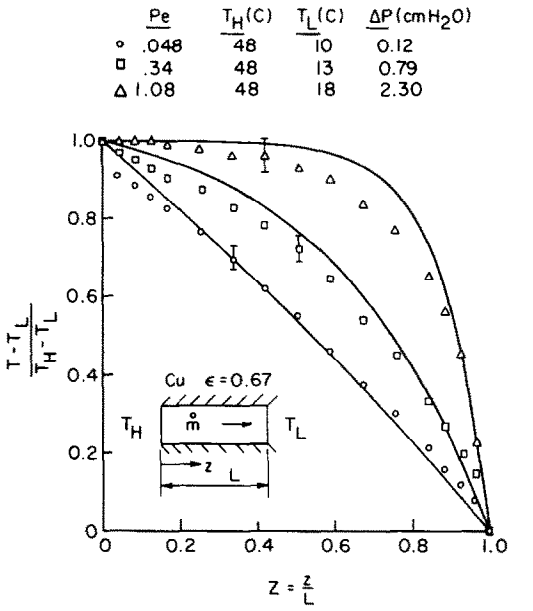

FIG. 5. Experimental and analytical axial temperature profiles for the copper specimen ($\varepsilon = 0.67$) for the insulated surface co-current flow case, see Fig. 1(A). The analytical profiles are the solid lines.

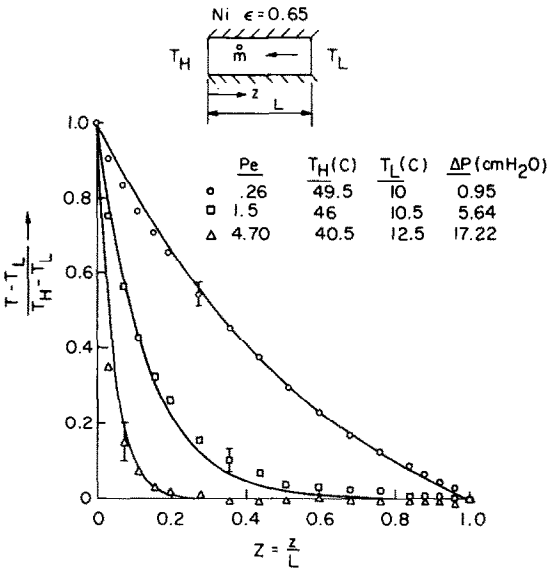

FIG. 6. Experimental and analytical axial temperature distributions for the Nickel 200 specimen ($\varepsilon = 0.65$) for the insulated surface counter current flow case, see Fig. 1(B). The analytical profiles are the solid lines.

Table 1. Test specimens and their properties

Specimen parent metal or alloy	Thermal conductivity of parent metal (W/m °C)	Measured porosity	Mean pore size* (cm)	Permeability (cm^2)	Measured λ_{eff} (W/m °C)	Temperature range for λ_{eff} (°C)
Copper	386	0.67	0.018	$2.03 \pm 0.12 \times 10^{-6}$	37.1 ± 2.9	5–55
Nickel 200	62	0.65	0.018	$6.03 \pm 0.42 \times 10^{-7}$	15.45 ± 1.24	5–55

*Data provided by manufacturer.

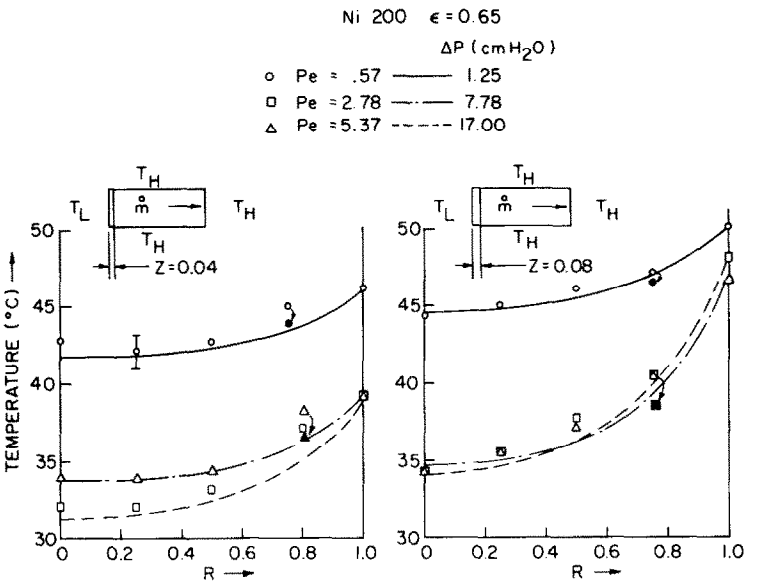

FIG. 7. Experimental and analytical radial temperature profiles for the Nickel 200 specimen ($\varepsilon = 0.65$) for the isothermal boundary condition, see Fig. 1(C). Two axial positions are shown $Z = 0.04$ and $Z = 0.08$. The solid lines are the analytical profiles. Open symbols are measured data and filled symbols are typical corrected data. The magnitude of the correction is indicated by curved arrow.

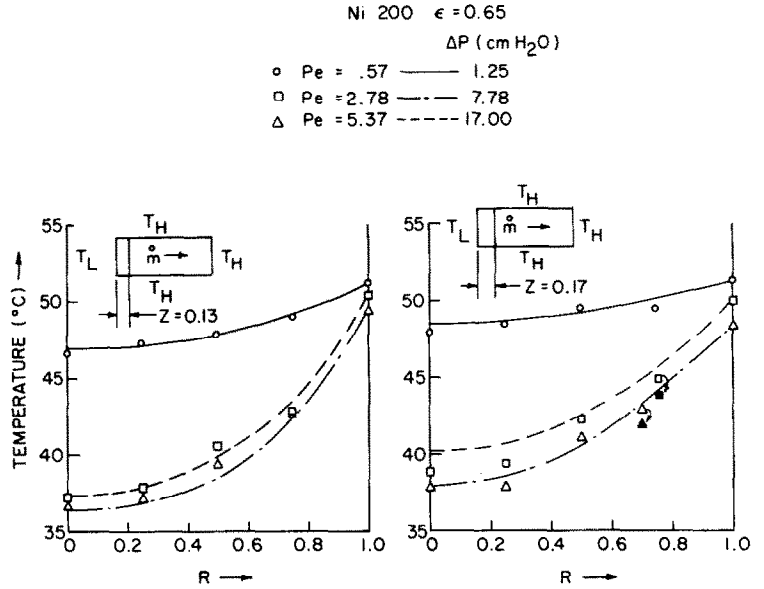

FIG. 8. Experimental and analytical radial temperature profiles for the Nickel 200 specimen ($\varepsilon = 0.65$) for the isothermal boundary condition, see Fig. 1(C). Two axial positions are shown $Z = 0.13$ and $Z = 0.17$. The solid lines are the analytical profiles. Open symbols are measured data and filled symbols are typical corrected data. The magnitude of the correction is indicated by curved arrow.

ductivity was measured using the apparatus discussed above with the steady state method of comparison as described in [2, 3, 19]. It is this effective thermal conductivity that is used in the analytical model. The reference velocity used in the Peclet number for the non-isothermal tests is

$$U_R = \frac{k(p_H - p_L)}{\frac{1}{2}(\mu_H + \mu_L)L}. \tag{18}$$

The coupled equations (12) and (13) are solved numerically subject to the appropriate boundary conditions by an explicit finite difference scheme using successive overrelaxation. A central difference scheme was used for the first order derivatives and a three point difference scheme was used for the second derivatives. The grid size was 8 (radial) by 48 (axial) and the accuracy of this scheme was of order $(1/48)^2$. This method was stable and in all cases converged within 150 iterations. The one dimensional case reduces to two coupled ordinary differential equations whereas the two dimensional case yields two coupled elliptic partial differential equations. The boundary conditions

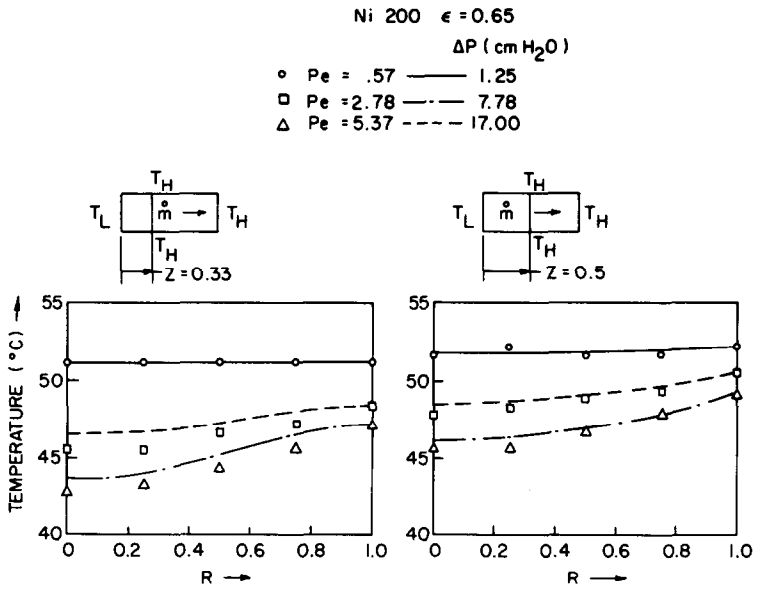

FIG. 9. Experimental and analytical temperature profiles for the Nickel 200 specimen ($\varepsilon = 0.65$) for the isothermal boundary condition, see Fig. 1(C). Two axial positions are shown $Z = 0.33$ and $Z = 0.5$. The solid lines are the analytical profiles.

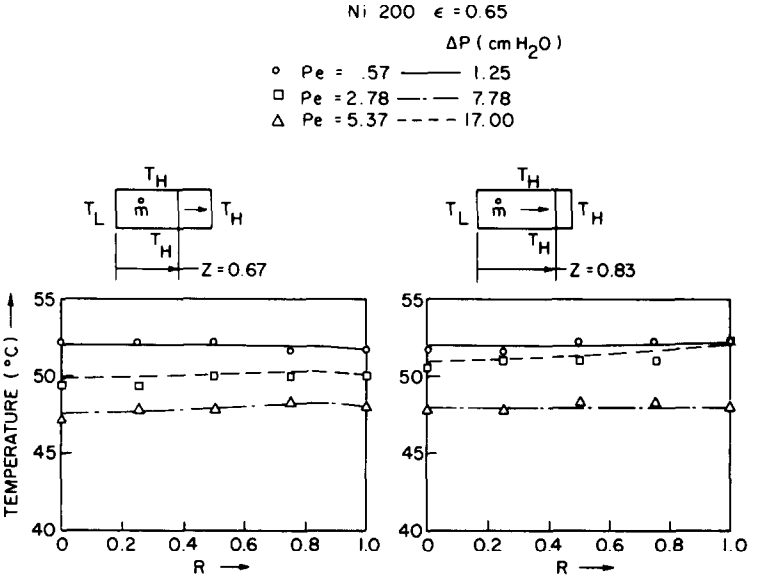

FIG. 10. Experimental and analytical radial temperature profiles for the Nickel 200 specimen ($\varepsilon = 0.65$) for the isothermal boundary condition, see Fig. 1(C). Two axial positions are shown $Z = 0.67$ and $Z = 0.83$. The solid lines are the analytical profiles.

[equations (15)–(17)] are mixed, i.e. both Dirichlet and Neuman. Hence an analytical solution becomes impractical. The solutions give the pressure, velocity and temperature distributions.

For the one dimensional cases, Fig. 1(A) and 1(B), the experimentally determined and analytically predicted axial temperature distributions are shown in Figs. 5 and 6. Figure 5 shows the co-current flow case for the copper specimen and Fig. 6 shows the counter current flow case for the nickel 200 specimen. The corresponding counter current flow case for the copper specimen and co-current flow case for the nickel 200 specimen show similar results. The solid lines are the numerical solutions and the data points are the experimental measurements. The agreement in all cases between the measured and predicted values is to within $\pm 9\%$.

Figures 7–10 show the comparison between the predicted and the measured temperature distributions for the nickel 200 specimen with the boundary conditions shown in Fig. 1(C). The temperature distribution is two dimensional. In this

case the radial temperature profiles are plotted at different axial distances. In each figure the different curves correspond to different Peclet numbers. Once again the solid or dotted lines represent the numerical solution whereas the measured values are shown by data points. The results for the copper specimen are similar. The agreement in all cases between the measured and predicted values is within $\pm 11\%$. In this case it should be pointed out that the thermocouples used to measure the temperature distribution in the specimen are radially inserted. Thus there is a temperature gradient along the thermocouples. This temperature gradient causes an error in the measured value because of conduction along the immersed portion of the thermocouple. An analysis of the error due to this effect is given by the authors in [20].

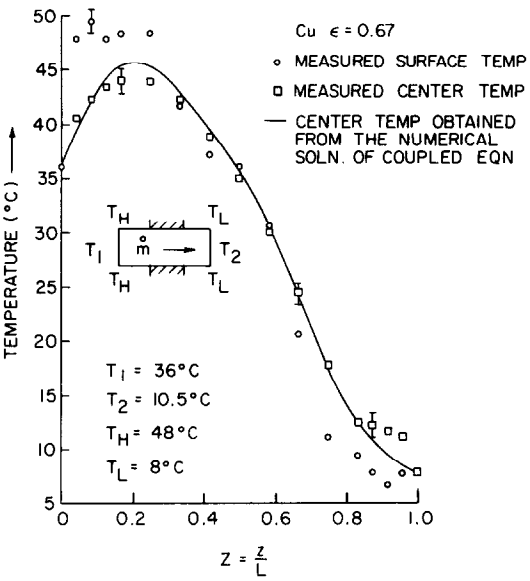

FIG. 11. Experimental and analytical temperature distributions for the copper specimen ($\varepsilon = 0.67$) at $r = 0$ for the heat pipe boundary condition, see Fig. 1(D).

Because of this effect the indicated or measured temperatures are higher than the true temperatures. The difference is proportional to the temperature gradient along the thermocouple. The temperature gradients are significant only near the inlet end ($z = 0$) of the specimen. Thus the errors are also only significant there and only data points in Figs. 8 and 9 had to be corrected. The open symbols in Figs. 7–10 indicate measured temperatures and the filled symbols in Figs. 8 and 9 indicate typical corrected data. The curved arrows indicate the magnitude of the correction.

Figure 11 shows a comparison of the measured and computed temperature profiles for the case of the copper specimen with the heat pipe boundary conditions, Fig. 1(D). In this case the temperature distribution is also two dimensional and the agreement in all cases between the measured and predicted values is to within $\pm 4\%$.

DISCUSSION AND CONCLUSIONS

This paper presents an experimental and analytical study of heat transfer and non-isothermal flow in sintered fiber metal wicks. Temperature distributions and pressure drops were measured in two metal wicks of copper (porosity, 0.67) and nickel 200 (porosity, 0.65) with water as the saturating fluid. Various flow and thermal boundary conditions were applied as shown in Fig. 1. The measured temperature distributions were compared to those predicted from the coupled momentum and energy volume averaged equations. This comparison showed that the agreement is very good, the maximum difference for all cases being $\pm 11\%$.

Thus the procedure presented in this paper for calculating the heat transfer of porous metals seems to be appropriate. The volume averaged conservation equations, equations (8) and (9) can be used to predict temperature distributions of saturated liquid flows in porous metals. These equations require the effective thermal conductivity of the saturated porous metal which was measured by the steady-state method of comparison.

Acknowledgements The authors are appreciative of the partial financial support for this work which was provided by the National Aeronautics and Space Administration through grants No. 36-003-064 and NSG 3040.

REFERENCES

1. R. L. Gorring and S. W. Churchill, Thermal conductivity of heterogeneous materials, *Chem. Engng Prog.* **57**, 28 (1961).
2. B. S. Singh, A. Dybbs and F. A. Lyman, Experimental study of the effective thermal conductivity of liquid saturated sintered fiber metal wicks, *Int. J. Heat Mass Transfer* **16**, 144 (1973).
3. K. Kar and A. Dybbs, Effective thermal conductivity of fully and partially saturated metal wicks, in *Heat Transfer* 1978, Vol. 3, edited by J. T. Rogers. Hemisphere, New York (1978).
4. J. C. Slattery, *Momentum, Energy and Mass Transfer*. McGraw-Hill, New York (1972).
5. A. Dybbs and S. Schweitzer, Conservation for non-isothermal flow in porous media, *J. Hydrology* **20**, 171 (1973).
6. A. E. Scheidegger, *The Physics of Flow through Porous Media*, 3rd Edn. University of Toronto Press, Toronto and Buffalo (1974).
7. A. Dybbs, Forced convection in a saturated porous medium, Ph.D. Thesis, University of Pennsylvania (1971).
8. H. Darcy, *Les Fontaines Publiques de la Ville de Dijon*. Victor Dalmont, Paris (1856).
9. S. Schweitzer, On a possible extension of Darcy's law, *J. Hydrology* **22**, 29 (1974).
10. B. S. Singh, B. Huang and A. Dybbs, Validity of Darcy's law for non-isothermal flow in porous media, Paper presented at A.I.Ch.E. Meeting, Houston, Texas, March (1975).
11. B. Huang and A. Dybbs, Mass and energy transport phenomena in porous media, FTAS/TR-75-111, Case Western Reserve University, Cleveland, Ohio (1975).
12. P. Forchheimer, *Z. Ver Dt., Ing.* **45**, 1782 (1901).
13. L. Green and P. E. Duwez, Fluid flow through porous metals, *J. Appl. Mech.* **18**, 39–45 (1951).
14. D. B. Greenberg and E. Weber, An investigation of the viscous and inertial coefficients for the flow of gases through porous sintered metals, with high pressure gradients, *Chem. Engng Sci.* **12** (1960).

15. G. S. Beavers and E. M. Sparrow, Non Darcy flow through fibrous porous media, *J. Appl. Mech.* **91**, 711–714 (1969).
16. J. C. Y. Koh, J. L. Dutton and B. A. Benson, Final report fundamental study of transpiration cooling, NASA CR-134528 (1973).
17. A. Dybbs and S. Schweitzer, Forced convection in a saturated porous medium, in *Heat Transfer* 1970, Vol. 7, edited by U. Grigull and E. Hahne, Section CT3/4, pp. 1–10. Elsevier, Amsterdam (1970).
18. B. S. Singh and A. Dybbs, Heat transfer characteristics of porous media, in *Heat Transfer* 1974, edited by T. Mizushina. Hemisphere, New York (1974).
19. B. S. Singh and A. Dybbs, Heat transfer and non-isothermal flow in porous media, FTAS/TR-75-106, Case Western Reserve University, Cleveland, Ohio (1975).
20. B. S. Singh and A. Dybbs, Error in temperature measurements due to conduction along the sensor leads, *J. Heat Transfer* **98**, 491 (1976).

ECOULEMENT D'UN LIQUIDE NON-ISOTHERME ET TRANSFERT THERMIQUE DANS DES MILIEUX POREUX METALLIQUES FRITTES

Résumé—On présente une étude expérimentale et théorique de l'écoulement d'un liquide non-isotherme dans un milieu poreux de fibres métalliques frittées. Le but est d'offrir une procédure pour déterminer les caractéristiques de transfert thermique des métaux poreux. On utilise les équations de bilan basées sur les moyennes volumiques. On admet la loi de Darcy et on suppose que l'équilibre thermique local existe entre le solide et le liquide. Les équations couplées de bilan sont résolues pour des distributions de température à une et deux dimensions en utilisant la méthode des différences finies. On considère différentes conditions aux limites pour l'écoulement et pour le problème thermique. Les expériences concernant la mesure des distributions de température et des conductivités thermique efficaces pour l'eau saturant des masses poreuses frittées de fibres de cuivre et de nikel. Les conductivités thermiques sont mesurées en utilisant la méthode de comparaison en régime permanent et les valeurs obtenues sont utilisées dans l'équation d'énergie. Les distributions mesurées de la température sont en accord avec celles calculées. Ainsi la procédure présentée, pour prévoir le transfert thermique, semble valide.

NICHT-ISOTHERME FLÜSSIGKEITSSTRÖMUNG UND WÄRMEÜBERTRAGUNG IN GESINTERTEN, METALLISCH PORÖSEN MEDIEN

Zusammenfassung—Mit dieser Arbeit werden eine experimentelle und eine analytische Untersuchung über die nichtisotherme Flüssigkeitsströmung in porösen, metallischen Medien aus gesinterten Fasern vorgelegt. Das Ziel der Arbeit ist, ein geschlossenes Verfahren zur Bestimmung der Wärmeübertragungseigenschaften von porösen Metallen vorzulegen. Bei der Analyse werden die Erhaltungssätze auf über das Volumen gemittelte Größen angewendet. Es wird angenommen, daß das Gesetz von Darcy gültig ist und daß zwischen der festen und flüssigen Phase örtlich thermisches Gleichgewicht besteht. Die gekoppelten, aus den Erhaltungssätzen resultierenden Gleichungen wurden mit Hilfe finiter Differenzenverfahren für ein- und zweidimensionale Temperaturverteilungen gelöst. Es wurden verschiedene Strömungs- und thermische Randbedingungen angenommen. Die Experimente umfassen die Messung von Temperaturverteilungen und effektiven Wärmeleitfähigkeiten von mit Wasser gesättigten Metalldochten aus gesinterten Kupfer- und Nickelfasern. Die effektiven Wärmeleitfähigkeiten wurden nach der stationären Vergleichsmethode gemessen und die erhaltenen Werte in der über das Volumen gemittelten Energiegleichung verwendet. Die gemessenen und die analytisch berechneten Temperaturverteilungen zeigen gute Übereinstimmung. Somit scheint das in dieser Arbeit angegebene Verfahren zur Berechnung der Wärmeübertragung gültig zu sein.

НЕИЗОТЕРМИЧЕСКОЕ ТЕЧЕНИЕ ЖИДКОСТИ И ПЕРЕНОС ТЕПЛА В МЕТАЛЛОКЕРАМИЧЕСКИХ ПОРИСТЫХ СРЕДАХ

Аннотация — В статье представлены результаты экспериментального и теоретического исследования неизотермического течения жидкости в агломерированных металловолокнистых пористых средах. Исследования проведены с целью получения надежной методики определения характеристик переноса тепла в пористых металлах. Для анализа использовались усредненные по объёму уравнения сохранения. Сделано предположение о справедливости закона Дарси и о локальном термическом равновесии между твердой и жидкой фазами. Связанные уравнения сохранения решались для случаев одномерного и двухмерного распределений температуры с использованием конечно-разностных схем и различных граничных условий. Экспериментально измерялись значения распределений температур и эффективной теплопроводности медных и никелевых металловолокнистых фитилей, насыщенных водой. При измерении эффективной теплопроводности применялся стационарный метод сравнения, а полученные результаты использовались в осредненном по объёму уравнении энергии. Отмечено хорошее совпадение экспериментальных и теоретических значений распределений температуры. Таким образом, предложенная в статье методика может быть использована для расчёта процесса переноса тепла.